European Journal of Pharmaceutical Sciences 202 (2024) 106897

Contents lists available at ScienceDirect

European Journal of Pharmaceutical Sciences

journal homepage: www.elsevier.com/locate/ejps

Mucoadhesive *in situ* nasal gel of amoxicillin trihydrate for improved local delivery: *Ex vivo* mucosal permeation and retention studies

Sandra Aulia Mardikasari [a,b], Gábor Katona [a,*], Mária Budai-Szűcs [a], Ágnes Kiricsi [c], László Rovó [c], Ildikó Csóka [a]

[a] Institute of Pharmaceutical Technology and Regulatory Affairs, Faculty of Pharmacy, University of Szeged, Eötvös St. 6, Szeged H-6720, Hungary
[b] Faculty of Pharmacy, Hasanuddin University, Makassar 90245, Indonesia
[c] Department of Oto-Rhino-Laryngology and Head-Neck Surgery, University of Szeged, Tisza Lajos krt. 111, Szeged H-6725, Hungary

ARTICLE INFO

Keywords:
Amoxicillin
In situ gelling
Bovine serum albumin
Gellan gum
Nasal delivery
Permeability study

ABSTRACT

Orally administered amoxicillin is recommended as the first-line treatment of acute bacterial rhinosinusitis (ABR) and given in a high-dose regimen. However, the risk of various systemic adverse reactions and low oral bioavailability are unbearable, increasing the threat of antibiotic resistance. Therefore, nasal delivery of amoxicillin can be a potential approach for effectively treating ABR locally, as well as overcoming those drawbacks. In a way to guarantee the effectiveness for local therapy in nasal cavity, the permeation and retention properties are of significant importance considerations. Accordingly, the present work aimed to investigate the characteristics with respect to the nasal applicability of the *in situ* gelling amoxicillin trihydrate (AMT) and further evaluate its permeability and retention properties through human nasal mucosa. The lyophilized formulations were characterized utilizing the Differential Scanning Calorimetry (DSC) and X-ray Powder Diffraction (XRPD), and also evaluated for its polarity, reconstitution time, droplet size distribution, mucoadhesive properties, and *ex vivo* permeability and retention studies. The results confirmed that the *in situ* gelling AMT formulations possess adequate mucoadhesive behavior, especially the formulation containing 0.3 % of gellan gum. Substantially, the *in situ* gelling AMT formulations were able to retain the drug on the surface of nasal mucosa instead of permeating across the membrane; thus, suitable for treating nasal infections locally. Altogether, the *in situ* gelling systems demonstrates promising abilities as a delivery platform to enhance local application of AMT within the nasal cavity.

1. Introduction

Amoxicillin (AMT) has been utilized as the first-line treatment for Acute Bacterial Rhinosinusitis (ABR) (Rosenfeld, 2016; Rosenfeld et al., 2015; Rovelsky et al., 2021; Snidvongs and Thanaviratananich, 2017). Conventionally, a solid dosage form (tablet) is used therapeutically in large doses for 7–14 days of treatment (Axiotakis et al., 2022; Lemiengre et al., 2018). As a consequence, various adverse reactions may take place, and the resistance threat is greatly unbearable. Futhermore, the absorption rate of orally administered high dose AMT indicated non-linearity in C_{max} therefore, low antibacterial efficacy (Huttner et al., 2020; Velde et al., 2016). To overcome these hurdles, the alternative route of administering antibiotics comes forward as an advantageous choice (Mardikasari et al., 2022b), which is suitable to deliver effectively the AMT to the target site, minimize the systemic adverse effect, and reduce the potency of antibiotic resistance threat (Nazli et al., 2022).

Intranasal delivery has emerged as a potential and valuable way of administering drugs. The nasal route administration confers multiple benefits, including the potential for localized nasal delivery, brain targeting, systemic drug delivery purposes, circumvention of first-pass metabolism, ease of application, and increased patient adherence (Keller et al., 2021). However, intranasal drug delivery also possesses some drawbacks, including nasal permeability, slightly acidic pH, small dosage volume, and the well-known challenge is to overcome the protective function of mucociliary clearance (MCC), which eliminates physiologically each exogenous materials within 15–20 min (Cingi et al., 2021). Hence, as an attempt to enhance the efficacy of therapy and ensure its prolonged effect, formulation strategy must be taken into consideration. The utilization of nanoparticles incorporated into a

* Corresponding author.
E-mail address: katona.gabor@szte.hu (G. Katona).

https://doi.org/10.1016/j.ejps.2024.106897
Received 28 March 2024; Received in revised form 2 September 2024; Accepted 4 September 2024
Available online 5 September 2024

stimuli-responsive *in situ* gelling polymer has been proven by many research groups to be able to retain the formulation in the nasal cavity and avoid rapid elimination due to nasal MCC while releasing the active ingredients (Chen et al., 2020; Emad et al., 2021; Huang et al., 2021a; Katona et al., 2020). Moreover, the integration of antibiotic substances into nanoparticulate delivery systems presents a markedly promising and efficacious avenue, offering great potential to mitigate the incidence of antibiotic resistance (Arana et al., 2021; Forier et al., 2014; Gao et al., 2014; Yeh et al., 2020; Zazo et al., 2016).

In line with this, albumin nanoparticles have been widely utilized as a promising vehicle for nasal delivery systems as they show many beneficial properties, including the specific binding sites for either hydrophilic or lipophilic drugs, higher entrapment efficiency, enhancing the solubility and stability of the drug, and the ability to generate a controlled release profile (Karimi et al., 2016; Kianfar, 2021; Loureiro et al., 2016; Singh et al., 2017). In addition, the incorporation of albumin nanoparticles into stimuli-responsive *in situ* gelling polymers can be employed as they have shown great potential and valuable results, which in this case is the ability to successfully deliver the drug for the desired therapeutic efficacy and enhance residence time in nasal cavity while extending the drug release (Agrawal et al., 2020; Katona et al., 2021; Mardikasari et al., 2022a; Protopapa et al., 2022; Verekar et al., 2020). Gellan gum (GG), one of the most extensively used polymers due to its ionic-responsive properties, is capable of undergoing a sol-to-gel phase transition upon nasal administration, attributable to the effect of nasal ionic conditions, especially Ca^{2+} (Cao et al., 2009; Gadziński et al., 2023), thus allowing the formulation to be retained in the nasal cavity and increase its residence time (Hao et al., 2016; Hosny and Hassan, 2014; Huang et al., 2021b).

In this regard, our research group has previously developed a nasal formulation of AMT-loaded albumin nanoparticle employing GG as an ionic-sensitive *in situ* gelling polymer through the application of Quality by Design methodology for enhanced treatment of local nasal infection (*i.e.*, ABR). This research exhibited promising results, and therefore, further additional investigation should be taken into account to evaluate its nasal applicability, especially its nasal mucosal permeation and retention properties (Mardikasari et al., 2023a).

Accordingly, present study aimed to characterize the *in situ* gelling formulation of AMT in a lyophilized form and investigate the critical properties related to its applicability for nasal delivery. Firstly, the prepared formulation of *in situ* gelling AMT was lyophilized, and then the physico-chemical properties of the lyophilized cakes were characterized utilizing Differential Scanning Calorimetry (DSC) and X-ray Powder Diffraction (XRPD). Subsequently, to evaluate the potential for nasal administration, the investigations were continued to determine the polarity of all *in situ* gelling AMT formulations through optical contact angle (OCA) measurements, the reconstitution time, the droplet size distribution, and the mucoadhesive properties on agar-mucin dish methods. Finally, all formulations of *in situ* gelling AMT were further evaluated for its *ex vivo* mucosal permeation and retention ability by employing human nasal tissues.

2. Materials and methods

2.1. Materials

Analytical grade amoxicillin trihydrate (AMT) was purchased from Thermo Fisher (Kandel) GmbH (Karlsruhe, Germany), bovine serum albumin (BSA, purity $\geq$ 97, lyophilized powder), low acyl gellan gum (Phytagel®), glucose anhydrous as crosslinker agent, agar 1 % solution, mucin from porcine stomach (Type II), ethanol 96 % v/v, and all other reagents were obtained from Merck Ltd. (Budapest, Hungary). Purified water was acquired through Gradient Water Purification System, the Millipore Milli-Q® (Merck Ltd., Budapest, Hungary). Analytical grade methanol was obtained from Molar Chemicals (Budapest, Hungary). All other chemicals used in this experiment were pharmaceutical grade.

2.2. Simulated nasal electrolyte solution preparation

Simulated nasal electrolyte solution (SNES) was prepared by weighing 0.59 g of anhydrous calcium chloride ($CaCl_2$), 2.98 g of potassium chloride (KCl), and 8.77 g of sodium chloride (NaCl). The mixture was then dissolved in 1000 ml of deionized water. The pH was adjusted to a final pH of 5.6 using 0.1 N NaOH or 0.1 N HCl (Sipos et al., 2021).

2.3. Preparation of in situ gelling formulation of AMT

The preparation of *in situ* gelling formulation of AMT was firstly started by fabricating the albumin-based nanoparticles of AMT and followed by incorporating into the *in situ* gelling polymer. The albumin-based nanoparticles of AMT was prepared according to our previous study (Mardikasari et al., 2023a). Initially, an accurately weighed amount of AMT (5 mg) was dissolved in purified water (0.9 ml). Subsequently, a 20% w/v solution of BSA (0.5 ml) was introduced and subjected to homogenization under continuous stirring at 500 rpm and a temperature of 37 °C, until a transparent solution was obtained. Then, ethanol 96 % v/v (0.8 ml) was added and the final mixture was heated to a temperature of 40 °C until a soft gel structure with opalescent appearance was observed, indicating the successful formation of BSA nanoparticles. Afterward, as crosslinker agent, 8% w/v of glucose (GLUC) was added to stabilize the resulting nanoparticles (Amighi et al., 2020).

Following this, specified amount of the *in situ* gelling polymer, GG, was uniformly dispersed and solubilized in purified water through heating at 90 °C (30 mins) (Salunke and Patil, 2016). After that, the obtained GG solution was cooled to ambient temperature. Subsequently, the prepared solution of albumin-based nanoparticles of AMT was slowly poured into the GG solution, following 1:1.5 vol ratio. The incorporation of albumin-based nanoparticles of AMT into GG solution as ionic-sensitive *in situ* gelling polymer was prepared in several concentrations, to achieve the final concentration of GG in the formulation as 0.2 %, 0.3 %, and 0.4 % w/v. Finally, the *in situ* gelling AMT formulations (GG0.2 %, GG0.3 %, and GG0.4 %) were then subjected to the lyophilization process by employing a ScanVac CoolSafe laboratory freeze-dryer (Labogene, Lynge, Denmark). This process was executed at a pressure of 0.013 mbar and a temperature of −40 °C over a period of 12 h, continued by a secondary drying stage at 25 °C for 3 h. The lyophilized samples were then preserved at 4 °C until further evaluations.

2.4. Characterization of the lyophilized in situ gelling formulation of AMT

2.4.1. Differential scanning calorimetry (DSC)

DSC measurements of all components of the formulation (AMT, BSA, GG, and GLUC) and the *in situ* gelling AMT formulations (GG0.2 %, GG0.3 %, and GG0.4 %) were performed utilizing a Mettler-Toledo DSC 3+ apparatus (Mettler-Toledo GmbH, Gießen, Germany), operating with temperature range of 25 to 300 °C at a controlled heating rate of 10 °C/min, under an inert argon which maintained at a flow rate of 150 ml/min. In this study, approximately 5 mg of all samples were placed into 40 µl aluminum pans. The obtained results were analyzed through STARe Software.

2.4.2. X-ray powder diffraction (XRPD)

XRPD diffractograms of all components of the formulation (AMT, BSA, GG, and GLUC) and the *in situ* gelling AMT formulations (GG0.2 %, GG0.3, and GG0.4 %) were recorded sing a BRUKER D8 Advance diffractometer (Bruker AXS GmbH, Karlsruhe, Germany). The diffractograms were acquired using a slit-detector Cu Kλ1 radiation (λ = 1.5406 Å). All samples were evaluated and scanned at a voltage of 40 kV and 40 mA, spanning an angular range of 3°–40° 2θ, with a step time of 0.1 s and a step size of 0.007° Sample analysis was performed in quartz

holder under conditions of room temperature and humidity.

2.4.3. Optical contact angel (OCA) measurement

The evaluation of wetting properties of the *in situ* gelling AMT formulations (GG0.2 %, GG0.3 %, and GG0.4 %), was performed using the OCA 20 Optical Contact Angle Measuring System (Dataphysics, Filderstadt, Germany) based on the Wu's harmonic mean equation (Kiss et al., 2022; Wu, 2007). A circular tablet of the pure GG as reference was compressed to a diameter size of 13 mm utilizing a hydraulic press (Specac Inc. Orpington, UK) with a force of 10 tons for 10 s. The solvents employed were distilled water with a polar surface tension (γ^p) of 50.2 mN/m and dispersive surface tension (γ^d) of 22.6 mN/m), and diiodomethane with a γ^p of 1.8 mN/m and a γ^d of 49 mN/m. The surface free energy (γ^*) was calculated by measuring the contact angle (θ) of both water and diiodomethane on the system using the sessile drop method. This procedure facilitated the determination of the interfacial tension of the polar component (γ_s^P) and dispersive component (γ_s^d) of the lyophilized *in situ* gelling AMT formulations, as delineated by following equation (Eq. (1)):

$$\gamma^* = \gamma_s^d + \gamma_s^p \tag{1}$$

Furthermore, the polarity of the lyophilized *in situ* gelling AMT formulations was quantified by calculating the ratio of the polar surface energy and the total surface energy, in accordance with equation (Eq. (2)):

$$Polarity\ (\%) = \frac{\gamma_s^p}{\gamma^*} * 100 \tag{2}$$

2.4.4. Determination of reconstitution time

Each formulation of *in situ* gelling AMT (GG0.2 %, GG0.3 %, and GG0.4 %) was reconstituted with 1.5 ml of purified water in order to reach the same concentration prior to the lyophilization process (AMT 1 mg/ml), and constantly stirred until no solid particles were visually observed. The time required to completely dissolve the lyophilized samples were recorded with stopwatch as the reconstitution time. The reconstitution times of all formulations were reported as means ± SD (Luoma and Lim, 2020; Taweel et al., 2021).

2.5. Viscosity measurement

The viscosity measurements were performed utilizing a rheometer instrument, RheoStress 1 HAAKE (Thermo Fisher Scientific, Karlsruhe, Germany). A thermostatic circulator (Thermo Haake Phoenix II + Haake C25P) was connected to the equipment to maintain the temperature during the measurement. In this experiment, a cone–plate geometry (radius: 49.9 mm, gap: 0.052 mm, angle: 1°) was used with a shear rate sweep of 0.01–100 s (Matricardi et al., 2009; Sanz et al., 2018; Sipos et al., 2020). The evaluation was carried out using a Haake RheoWin® Job Manager v.3.3 software (Thermo Electron Corporation, Karlsruhe, Germany). Following this, the obtained data were processed using a Haake RheoWin® Data Manager v.3.3 software (Thermo Electron Corporation, Karlsruhe, Germany). All measurements were carried out in triplicate at 34 °C and the results were reported as the average ± SD.

2.6. Determination of droplet size distribution

The measurement of droplet size distribution of all *in situ* gelling AMT formulations (GG0.2 %, GG0.3 %, and GG0.4 %) was performed utilizing laser diffraction technique. This analysis was conducted with a Malvern Spraytec® system (Malvern Instruments Ltd., Malvern, UK), equipped with a 300 mm lens that capable of analyzing droplet sizes in a range of 0.1 − 900 μm (Dv 50: 0.5 − 600 μm) (Jullaphant et al., 2019; Kundoor and Dalby, 2011; Pu et al., 2014). The nasal spray device tip was aligned and positioned horizontally with the receiving lens, ensuring the laser beam precisely intersected with the center of the spray cone's expansion. The measurements were performed at room temperature. Initially, the *in situ* gelling AMT formulations (0.2 %, 0.3 %, and 0.4 % of GG) were reconstituted with 1.5 ml of purified water and subsequently transferred into a nasal spray container. Manual actuation of each nasal spray was performed thrice and discharged into waste, allowing the device for a prime condition. Following this, three repeated test actuations on different batches were carried out. The data were analyzed using Spraytec software v4.00 (Malvern Panalytical Ltd., Malvern, UK), with the volume diameter and described as 10 % (*Dv10)*, 50 % (*Dv50)*, and 90 % (*Dv90)* of the cumulative volume distribution. Span was quantified according to the equation below (Eq. (3)):

$$Span = \frac{(Dv90 - Dv10)}{Dv50} \tag{3}$$

2.7. Evaluation of mucoadhesive properties

The mucoadhesive properties of the *in situ* gelling AMT formulations were evaluated by two distinct methods: the displacement method and the flow-through method. At first, approximately 100 g of hot solution containing 1% w/v agar with 2% w/v mucin in purified water was casted onto a petri dish (diameter 10 cm) and left to solidify for 12 h at 4 °C. After that, prior to the test, the petri dishes were then stored at 34 °C for 1 h, to equilibrate following experimental condition. Subsequently, 1 ml of each formulation and as reference AMT aqueous solution (1 mg/ml) were placed on top of the agar-mucin gel. Finally, for the displacement methods (Lungare et al., 2016; Trenkel and Scherließ, 2021; Youssef et al., 2018; Yu et al., 2023), all petri dishes were oriented at a 60° angle, allowing the samples to move downwards (displacement). The displacement distance was measured in centimeters for up to 2 h, with the adhesion potential being inversely proportional to the sample's displacement. On the other hand, for the flow-through method (Chen et al., 2018; Cook et al., 2017; Khutoryanskiy, 2011; Syed et al., 2022), a modified apparatus was utilized. All petri dishes were inclined at a 60° angle, and the flow of the SNES was maintained through a peristaltic pump with a flow rate of 2 mm/min (Illum, 2006; Inoue et al., 2018) to wash off the formulation from the surface of agar-mucin gel. 1–1 ml aliquots of the wash-out solution was collected at pre-determine time points (3, 5, 10, 15, 20, and 30 min). Prior to drug content determination with HPLC, aliquots were freeze-dried and dissolved in 100 μl purified water to ensure that the concentration of analyte reached the limit of detection (LOD). The measurements were performed in triplicate and reported as means ± SD.

2.8. Ex vivo mucosal permeation study

Ex vivo mucosal permeation study was carried out using human nasal mucosa or mucoperiosteum (Sipos et al., 2023). The experimental protocol was approved by the institutional ethics committee of the University of Szeged (ETT-TUKEB: IV/3880–1/2021/EKU). Nasal mucosa tissue samples were procured during the routine nasal and sinus surgical procedures (septoplasty), performed under either general or local anesthesia. Briefly, a local injection of 1% *w/v* lidocaine-Tonogen was given to secure the nasal surgical area. Then, the mucosa was elevated from the nasal base using a Cottle elevator or raspatorium. After that, the obtained nasal mucosa tissue was transported from the surgical facility to the laboratory in a maintained condition using a physiological saline solution, and the experiment was immediately performed.

The permeation study was executed employing a modified Side-Bi-Side® type horizontal permeation apparatus as shown in Fig. 1, featuring a diffusion surface area of 0.785 cm^2. The nasal mucosa tissue was cut and excised using a surgical scalpel and affixed between the donor and acceptor compartments. The donor medium was 1 ml of AMT solution (1 mg/ml) and *in situ* gelling AMT formulation, diluted with 8 ml of SNES. Conversely, the acceptor compartment was filled with 9.0

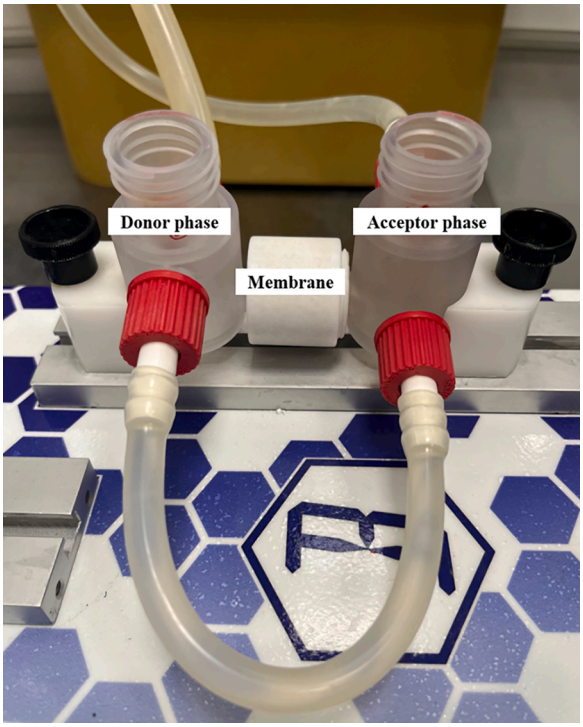

Fig. 1. Illustration of Side-Bi-Side® permeation apparatus.

ml of PBS (pH 7.4 ± 0.1). Temperature was maintained at 34 ± 2 °C using a ThermoHaake C10-P5 heating circulator (Sigma–Aldrich Co., Ltd., Budapest, Hungary) and stirred at 100 rpm continuously. Sequentially, at 60 min, aliquots (150 µL) from the acceptor chamber were withdrawn. Prior to drug content determination with HPLC, aliquots were freeze-dried and dissolved in 75 µl purified water to ensure that the concentration of analyte reached the limit of detection (LOD).

The apparent permeability (P_{app}) of AMT across the nasal mucosa at 60 min was quantified using the following equation (Keller et al., 2021):

$$P_{app}(cm/s) = \frac{\Delta[C]_A \times V_A}{A \times [C]_D \times \Delta t} \quad (4)$$

where, ($\Delta[C]_A$) is the concentration differential of AMT in the acceptor chamber after the experiment (60 min), V_A is the volume of the acceptor chamber (9 ml), A is the surface area of permeability test (0.785 cm^2), ($[C]_D$) is the initial concentration of AMT in the donor compartment at time point zero and t is the incubation time (s).

2.9. Ex vivo recovery and extraction assays

The recovery and extraction assays were performed by measuring the amount of AMT retained in the nasal mucosa following the *ex vivo* permeation studies. After completing the *ex vivo* permeation test, the nasal tissue membrane was taken and weighted. Subsequently, the nasal tissue membrane was soaked with 2 ml methanol-water (1:1) and placed on an orbital shaker (PSU-10i Orbital Shaker, Grant Instruments Ltd, Cambs, England) for 60 min at 450 rpm to extract the retained AMT. Prior to AMT content determination with HPLC, aliquots were freeze-dried and dissolved in 100 µl methanol-water (1:1) to ensure that the concentration of analyte reached the limit of detection (LOD) (Enggi et al., 2021; Permana et al., 2021; Sanz et al., 2018).

2.10. Ex vivo retention study by Raman chemical mapping

Retention study utilizing Raman chemical mapping was conducted to visually analyze the AMT which retained in the human nasal tissues following the *ex vivo* permeation studies (Katona et al., 2022). The nasal tissue membrane was sectioned at 20 µm thickness using microtome (Leica CM1950 Cryostat, Leica Biosystems, Wetzlar, Germany) and put on an aluminum foil-covered glass slide as a sample holder. Raman mapping of cross-sectioned mucosa was carried out utilizing a DXR Raman Microscope (Thermo Fisher Scientific Inc., Waltham, MA, USA), which was outfitted with a charge-coupled device (CCD) camera. Raman maps were acquired from a 100 × 1000 µm surface with a step resolution of 50 µm (60 spectra). This process employed a 780 nm diode laser with an output power of 12 mW and utilized a 50 µm slit aperture. Each spectral scan was conducted for over 2 s, following a preliminary 2 s laser exposure and the spectrum represented the average of 32 scans within the spectral domain of 3300–200 cm^{-1}. Furthermore, cosmic ray and fluorescence correction were applied in order to decrease the signal-to-noise ratio. The distribution of AMT in the sectioned tissue was determined by using the Raman spectrum of pure AMT as a profile. Raman maps were evaluated through OMNIC 8.3 software (Thermo Fisher Scientific Inc., Waltham, MA, USA).

2.11. HPLC analysis

The quantification of AMT within the *in situ* gelling formulation was conducted using HPLC Agilent Infinity1260 (Agilent Technologies, Santa Clara, CA, USA). The chromatographic separation was achieved on a Kinetex® EVO C18 100 Å column (150 mm × 4.6 mm, 5 µm particle size; Phenomenex, Torrance, CA, USA). In this investigation, analytical samples of 10 µL were injected into the HPLC system and maintained at a column temperature of 25 °C. The mobile phase consisted of 25 mM phosphate buffer (pH 4.6) (A) and methanol (B), delivered at a flow rate of 1 ml/min. A gradient elution program was employed over 5 min, commencing with 95 % (A) for the initial 2 min, followed by a reduction to 75 % (A) for the subsequent 2 min, and concluding with a return to 95 % (A) for the final minute. Detection was performed at a wavelength of 230 nm utilizing a UV–VIS diode array detector. Data analysis was facilitated by Chem-Station software version B.04.03 (Agilent Technologies, Santa Clara, CA, USA). The retention time for AMT was established at 2.5 min, and the calibration curve exhibited a regression coefficient (R^2) of 1.0 within the concentration range of 100–1000 µg/ml. The LOD was 89.38 µg/ml, while the limit of quantification (LOQ) was 270.84 µg/ml.

2.12. Statistical analysis

The collected data were presented as means ± standard deviation (SD). Statistical analysis were conducted utilizing GraphPad Prism® software version 8 (GraphPad Software, San Diego, CA, USA) and TIBCO Statistica® 13.4 (Statsoft Hungary, Budapest, Hungary). One-way analysis of variance (ANOVA) was employed to evaluate statistical significance within the *ex vivo* permeability study for comparing the results. Moreover, a p value of <0.05 was considered significant.

3. Results and discussion

3.1. Characterization of the lyophilized in situ gelling AMT formulation

3.1.1. DSC study

The DSC thermograms of the formulation components (AMT, BSA, GG, and GLUC) and the *in situ* gelling AMT formulations (GG0.2 %, GG0.3 %, and GG0.4 %) are depicted in Fig. 2. The thermogram of AMT exhibited a characteristic endothermic peak at 127 °C, emphasizing the loss of crystalline water from AMT, however, this peak was shifted to a higher temperature (140−143 °C) in the case of GG0.2 %, GG0.3 % and GG0.4 %, indicating the gel matrix of the formulation hindered the elimination of crystalline water. Furthermore, the thermogram of AMT also showed an exothermic peak at 182 °C, which indicates the decomposition temperature (Obaidat et al., 2022). This peak is missing

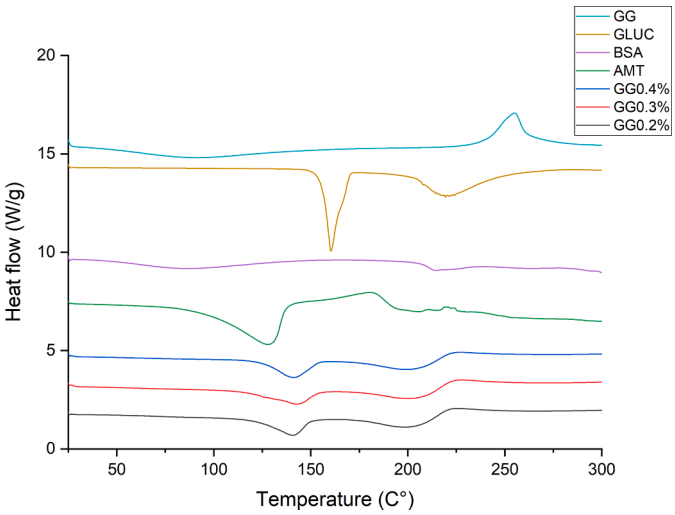

Fig. 2. DSC Thermogram of the formulation components: AMT – amoxicillin trihydrate, BSA – bovine serum albumin, GG – gellan gum, and GLUC – glucose; and all formulations of the *in situ* gelling AMT: GG0.2 %, GG0.3 %, and GG0.4 %.

from the thermogram of GG0.2 %, GG0.3, and GG0.4 %, suggesting improved thermal stability of the drug. Another endothermic peak of AMT was found at 198 °C which belongs to its melting point, and can also be found in the formulation of GG0.2 %, GG0.3, and GG0.4 %, indicating the presence of the drug in crystalline form in all formulations. The thermogram of GLUC exhibited a characteristic endothermic peak at 160 °C which indicates its melting point (Hurtta et al., 2004); however, in the thermogram of GG0.2 %, GG0.3 %, and GG0.4 % this peak cannot be observed due to the amorphization of GLUC during lyophilization process.

3.1.2. XRPD investigation

XRPD diffractograms of all components in the formulation (AMT, BSA, GG, and GLUC) and the *in situ* gelling AMT formulations (GG0.2 %, GG0.3 %, and GG0.4 %) are expressed in Fig. 3. The main characteristic peaks of AMT as strong and sharp peaks are located at 2θ of 12.12°, 15.14°, 18.04°, 19.31°, 25.74°, 26.68°, and 28.69° which presents its crystalline nature. However, the characteristic peaks of AMT are missing from the diffractogram of GG0.2 %, GG0.3 %, and GG0.4 %, confirming

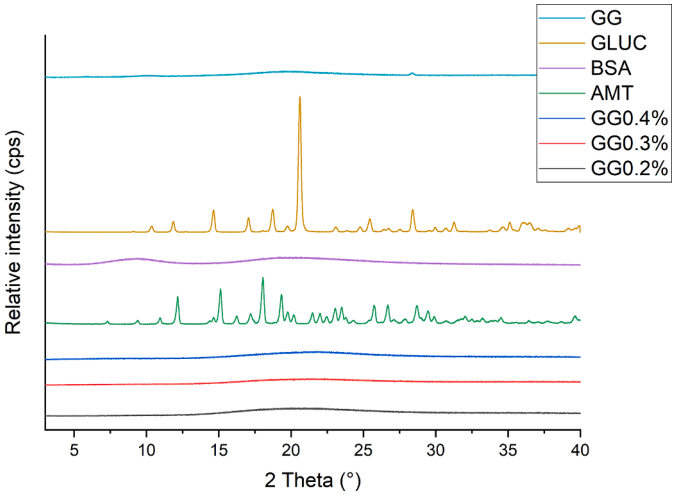

Fig. 3. XRPD diffractogram of the formulation components: AMT, BSA, GG, and GLUC; and all formulations of the *in situ* gelling AMT: GG0.2 %, GG0.3 %, and GG0.4 %.

that the AMT was successfully entrapped in the amorphous GG-BSA gel matrix in the formulation. This result conforms to the result of DSC which revealed that AMT can be found in crystalline form in the formulation of *in situ* gelling AMT, the GG0.2 %, GG0.3 %, and GG0.4 %. Moreover, the diffractogram also denoted the characteristic peaks of GLUC at 2θ of 14.64°, 17.05°, 20.61°, and 28.41° The absence of characteristic GLUC peaks in the diffractogram of GG0.2 %, GG0.3 %, and GG0.4 % also supports that the GLUC went through amorphization during the lyophilization process.

3.1.3. Wettability studies

The measurement of contact angle serves as an assessment of a liquid's capacity to wet a solid substrate, with lower contact angle values indicates a superior wetting characteristics (Kulkarni et al., 2018). Contact angle is directly associated with surface free energy in which a higher surface free energy can particularly cause a good wetting behavior and highly affected by the polarity or hydrophobicity of the liquid. Good wettability of a lyophilized sample is essential for facilitating penetration process of the reconstitution fluid through the matrix interior. Nonetheless, while wettability is a critical initial step, it is not the sole factor influencing the duration of the reconstitution process (Kulkarni et al., 2018).

In the present work, the wetting properties investigation of the lyophilized *in situ* gelling AMT formulation, as provided in Table 1, revealed that by increasing the GG concentration, the polarity of the lyophilized samples decreased, which can be claimed with the less polar behavior of the initial GG. Substantially, the used GG in this experiment which is a low-acyl GG, is an anionic polysaccharide composed of a tetra-saccharide repeating unit with low acetyl content and requires a high temperature to be fully dispersed in water (Cassanelli et al., 2018; Fiorica et al., 2021). Hence, the polarity of the initial GG was found to be lower than all formulations of *in situ* gelling AMT. In terms of this, the BSA and GLUC content in the formulations has a role as the hydrophilic components, thereby raising the polarity of *in situ* gelling AMT formulations. In addition, it has been previously studied that sugar molecules can improve wettability of the cake solid, allowing easier cake disintegration in the lyophilized product (Cao et al., 2013; Kulkarni et al., 2018).

Further, a decreasing polarity was observed for all lyophilized samples of *in situ* gelling AMT formulations which contain 0.2 %, 0.3 %, and 0.4 % of GG, with a proportionally decreasing trend depending on the GG concentration. Since various GG concentrations demonstrated different polarity, the water absorption capacity of each formulation can particularly be affected, which then potentially generates variations in the reconstitution time (Luo et al., 2021).

3.2. Reconstitution time

Reconstitution process is a significant factor influencing the application of pharmaceutical products which are stored in solid form and need to be reconstituted before use, as the liquid form has more

Table 1
Contact angle, surface free energy, and polarity of the lyophilized *in situ* gelling AMT formulations and the initial GG. Data are shown as means ± SD, $n = 3$.

Surface	Θ_{water} (°)	$\Theta_{diiodomethane}$ (°)	γ_s^d (mN/m)	γ_s^p (mN/m)	γ^* (mN/m)	Polarity (%)
GG	40.97 ± 2.85	7.31 ± 2.66	25.32	45.59	70.91	35.71
GG 0.2 %	35.17 ± 2.37	24.41 ± 2.45	29.05	41.84	70.89	59.02
GG 0.3 %	18.3 ± 1.78	27.18 ± 2.08	35.89	40.87	76.76	53.24
GG 0.4 %	22.81 ± 2.84	35.67 ± 2.43	35.66	37.69	73.35	51.38

therapeutic potential. Long reconstitution times not only cause inconvenience to the patient, but can also pose a safety risk if the product is administered before all solids are completely disintegrated or redispersed. A short reconstitution time results from the reconstitution fluid penetrating the freeze-dried cakes more effectively due to good wettability, polarity, and a more open pore network (Beech et al., 2015).

Based on the results as shown in Fig. 4, the lyophilized samples of *in situ* gelling AMT formulation (GG0.2 %, GG0.3 %, and GG0.4 %) showed complete dispersion with a reconstitution time of 4.09 ± 0.5, 6.18 ± 1.2, and 9.23 ± 1.5 min, respectively. These results demonstrated that the higher the polymer (GG) content, the longer the reconstitution time. As the polymer (GG) has a quite low polarity as mentioned in the previous section, then the formulation with higher GG concentration particularly required more time to completely redisperse the lyophilized *in situ* gelling AMT formulations. Particularly, reconstitution process involves some steps related to the lyophilized cakes attributes, including the wettability, penetration process of the reconstitution fluid into the lyophilized cakes, and dispersibility behavior (Beech et al., 2015; Kulkarni et al., 2020). Therefore, the higher concentration of polymer (GG) in the formulation (*i.e.*, GG0.4 %) which may perform a more packed and entangled structure, required longer time for the rehydration process compared to the other formulations (Beech et al., 2015; Kulkarni et al., 2020; Luo et al., 2021; Luoma and Lim, 2020).

3.3. Viscosity measurement

For the viscosity (η) results, as illustrated in Fig. 5, the viscosity of all *in situ* gelling AMT formulations (GG0.2 %, GG0.3 %, and GG0.4 %) before the sol-to-gel transition showed quite low viscosity values and it can be confirmed that the viscosity increased along with the increasing amount of polymer (GG) in the formulation. Interestingly, the viscosity behavior can directly affect the droplet size of the nasal spray product and its nasal deposition (Scherließ, 2020). In this case, an *in situ* gelling formulation with a low viscosity nature before the administration into the nasal cavity could potentially generate uniformity of the delivered dose, allowing an easier spraying process and ultimately supporting its nasal applicability.

Moreover, the results in Fig. 5 revealed that as the shear rate increased from 0 to 100 s-1, the *in situ* gelling AMT formulations (GG0.2 %, GG0.3 %, and GG0.4 %) experienced a decrease in the viscosity value, demonstrating a non-Newtonian pseudoplastic behavior. Notably, this pseudoplastic characteristic is preferable for nasal formulations as it facilitates less dripping from the nasal cavity; thus, in terms of *in situ* gelling formulation, it might support the proper sol-to-gel transition once the formulation in contact with nasal environment. In this circumstances, viscosity plays important role in nasal formulation, in which it can affect the droplet size of the spray, drug deposition and retention time, as well as drug absorption through nasal mucosa (Furubayashi et al., 2007; Scherließ, 2020).

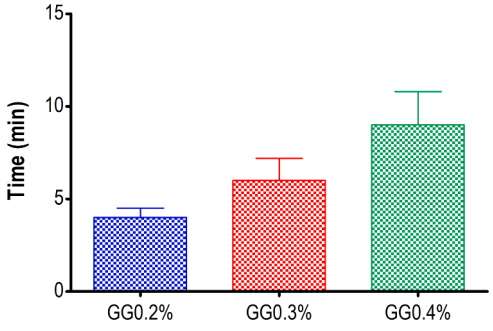

Fig. 4. Reconstitution time of all *in situ* gelling AMT formulations: GG0.2 %, GG0.3 %, and GG0.4 %. Data are shown as means ± SD, $n = 3$.

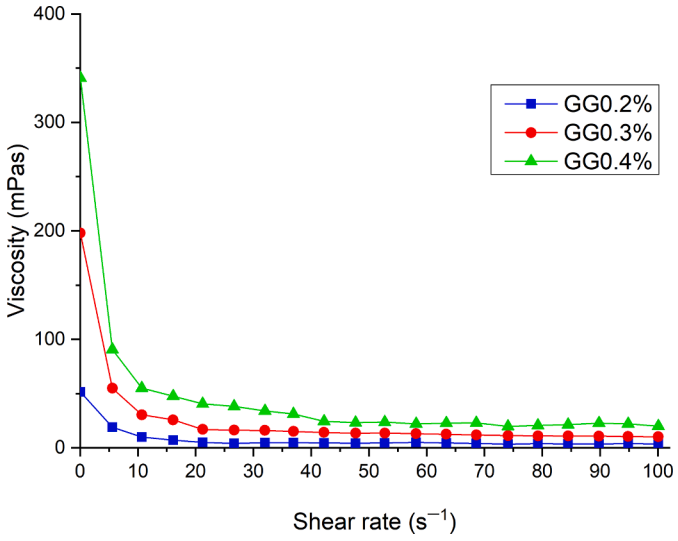

Fig. 5. Viscosity curve of all *in situ* gelling AMT formulations: GG0.2 %, GG0.3 %, and GG0.4 %. Data are shown as means ± SD, $n = 3$.

3.4. Droplet size distribution of the in situ gelling AMT formulation

Droplet size distribution (DSD) is a pivotal parameter for nasal sprays, as it profoundly impacts the deposition of the therapeutic agent within the nasal cavity (Djupesland and Skretting, 2012; Le Guellec et al., 2021), which can ultimately affect the efficacy of a product. Moreover, in order to ensure adequate retention of the formulation within the nasal passage, the cutoff points for the droplet sizes should adhere to the FDA's specification range for nasal spray products, which is 30 − 120 μm (Trows et al., 2014). The droplet size which are too small (<10 μm), can pass through the nasal cavity and enter into the lung, resulting in ineffectiveness of nasal sprays (EMA, 2006; Gao et al., 2020; Gholizadeh et al., 2019). The results of droplet size measurement, as shown in Table 2, exhibited that the droplet size of *in situ* gelling formulations of AMT varies. However, obtained droplet size distribution of the formulation with GG0.3 % was in agreement with the guidelines. Moreover, it was found that the formulation with GG0.4 % showed the largest droplet size of all, which might be due to its higher polymer concentration that provides greater cohesive forces. On the other hand, the formulation with GG0.2 % showed a quite opposite results, in which a much bigger droplet size than the formulation with GG0.3 % was observed, while the polymer concentration was lower. This phenomenon might be attributed to the actuation force's impact on the nasal spray product's and the formulation's shear-thinning properties (Dayal et al., 2004; Trows et al., 2014). Moreover, according to the result of Span value, the formulation of GG0.3 % seems appropriate, as the smaller the number, the less variation there is between the size of the droplets in the spray spectrum (Chen and Ashgriz, 2022; Kramm et al., 2023).

Table 2
Droplet size distribution parameters of all *in situ* gelling AMT formulations. Data are shown as means ± SD, $n = 3$.

Formulations	Dv10 (μm)	Dv50 (μm)	Dv90 (μm)	Span
GG0.2 %	57.74 ± 2.72	108.05 ± 5.39	233.10 ± 25.70	1.69 ± 0.19
GG0.3 %	53.01 ± 5.07	82.80 ± 7.63	136.52 ± 17.60	0.97 ± 0.16
GG0.4 %	64.22 ± 10.02	150.85 ± 23.98	515.76 ± 66.39	2.84 ± 0.54

3.5. Evaluation of mucoadhesion properties

The evaluation of mucoadhesion properties of the *in situ* gelling AMT formulation was assessed by two modified methods, namely the flow-through and the displacement method. The results of the flow-through method, as illustrated in Fig. 6, showed that the washed amount of AMT from all samples increased by the time. The higher washed amount was generated by AMT 1 mg/mL solution as control, due to its liquid state that made it directly move downward once placed on the surface of the inclined agar-mucin gel. Also, the SNES droplets leaving the peristaltic pump allowing the AMT solution to be pushed downward without being retained on the surface of the agar-mucin gel.

Furthermore, the *in situ* gelling AMT formulations (GG0.2 %, GG0.3 %, and GG0.4 %) exhibited a lower washed amount of AMT in comparison to the AMT solution. According to the results, the washed amount of AMT tends to be proportional to the concentration of GG in the formulation. The higher the GG concentration, the lower the amount of AMT obtained after washed off process. This can be explained through the mechanism in which the SNES droplets from peristaltic pump promote ionic condition (providing Ca^{2+}) that immediately facilitate the sol-gel transformation of GG in the formulation, resulting in a higher viscosity solution that is able to be retained on the surface of agar-mucin gel (Kolawole and Cook, 2023). Moreover, the mucoadhesive properties were also supported by the interaction between the BSA content in the *in situ* gelling formulations of AMT with the mucin in the agar mixture. The BSA plays an important role for the interaction with mucin, due to its high binding affinity to the mucin, which known as BSA-mucin binding (del Castillo-Santaella et al., 2022; Kakati et al., 2022; Mardikasari et al., 2023b). Accordingly, the *in situ* gelling AMT formulations can definitely attach to the surface of agar-mucin gel, that indicates high mucoadhesive potential, resulting in a lower amount of washed-out AMT.

In addition, for the displacement method, the results as shown in Table 3 exhibited a quite similar results with the previously mentioned method. The AMT control directly moved downward while placed on the surface of inclined agar-mucin gel, due to its behavior as a liquid solution. Meanwhile, the formulations of *in situ* gelling AMT formulations showed interesting displacement results for up to 2 h of investigation. The formulation of GG0.2 % showed a higher displacement distance of about 5.5 ± 0.2 cm, compared to GG0.3 % and GG0.4 % with approximately 1.6 ± 0.3 cm and 1.1 ± 0.2 cm, respectively. These results reflect good adherence and recorded as good mucoadhesion potential. Overall, the evaluation of mucoadhesive properties demonstrated that the *in situ* gelling AMT formulations have the potential to adhere to the nasal wall once instilled to the nasal cavity and would not be easily washed out, allowing the formulation to be retained to the nasal mucosa and release the drug.

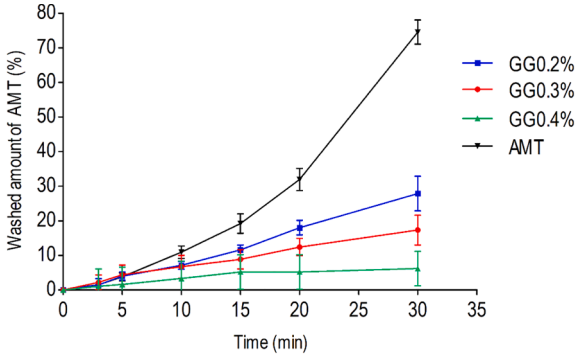

Fig. 6. The flow-through method, illustrating the washing resistance of all *in situ* gelling AMT formulations (GG0.2 %, GG0.3 %, and GG0.4 %) in comparison to the AMT solution (1 mg/ml) as control. Data are shown as means ± SD, $n = 3$.

Table 3
Displacement distance of the *in situ* gelling AMT formulations and AMT solution. Data are shown as means ± SD, $n = 3$.

Formulation	AMT solution (1 mg/ml)	GG0.2 %	GG0.3 %	GG0.4 %
Displacement after 2 h (cm)	-*	5.5 ± 0.6	1.6 ± 0.3	1.1 ± 0.8

* Not measurable, directly flows downwards.

3.6. Ex vivo mucosal permeation study

Ex vivo permeation study of the *in situ* gelling AMT formulations and aqueous AMT solution (1 mg/ml) were executed using a modified Side-Bi-Side® type permeation cell using human nasal mucosa. The Side-Bi-Side® type horizontal diffusion cell is widely recommended for the investigation of nasal liquid preparations (Bartos et al., 2021) as in present case for the *in situ* gelling AMT formulations. In this circumstance, the apparent permeability coefficient (P_{app}) is suitable parameter to characterize the nasal penetration of drug. Fig. 7 shows the P_{app} value of the AMT solution was also significantly higher ($p < 0.05$) compared to the *in situ* gelling AMT formulations, moreover the GG0.4 % indicates significantly lower ($p < 0.05$) P_{app} value in comparison to GG0.2 %. This parameter was inversely proportional to the GG concentration, an increased gel strength by increasing the GG concentration in the formulations resulted in higher retention of AMT in the gel matrix, supporting the application for local therapeutic effect and hindered systemic absorption (Kolawole and Cook, 2023).

3.7. Ex vivo recovery and extraction assays

The aim of this work was to develop *in situ* ionic sensitive gel of AMT for local therapy in nasal cavity. In this circumstance, the AMT was intended to be retained in the nasal mucosa instead of permeate through the membrane. Therefore, it is important to investigate the amount of AMT retained in the nasal mucosa, in order to evaluate the ability of the formulation to hold the drug in the gel matrix, which further greatly influence the efficacy of the treatment. The results showed that GG0.4 % showed the lowest amount of AMT, approximately 0.180 μg/mg. This demonstrated that the drug was entrapped in the gel matrix of GG0.4 % formulation and because of its high viscosity, then the AMT was not able to permeate to the nasal mucosa. Moreover, higher amount of AMT was found on the nasal mucosa for GG0.3 % and GG0.2 %, which were

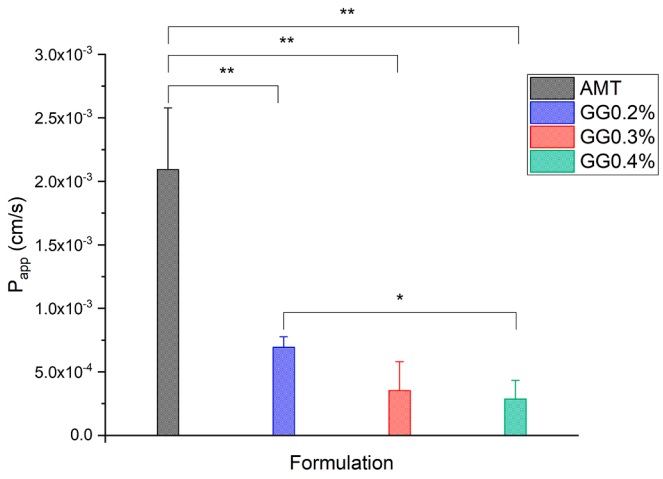

Fig. 7. Apparent permeability of the *in situ* gelling AMT formulations: GG0.2 %, GG0.3 %, and GG0.4 %; compared to the AMT solution (1 mg/ml) as control during 60 min of treatment. Data are shown as means ± SD, $n = 3$. Significant differences are indicated with asterisks ($*p < 0.05$ and $**p < 0.01$).

around 0.298 μg/mg and 0.378 μg/mg, respectively, compared the AMT solution as control with 3.314 μg/mg amount of retained AMT. These findings were also in line with previous results of *ex vivo* permeation studies, as presented by the low amount of drug permeated and inversely proportional to the GG concentration used in the formulation. Hence, this investigation indicated the potential of the *in situ* ionic sensitive gel of AMT formulation to retain the drug locally in the nasal tissue.

3.8. Ex vivo retention test by Raman chemical mapping

Raman chemical mapping was utilized to investigate the retention properties of the *in situ* gelling AMT formulation in order to ensure its applicability is suitable for the treatment intended for localized effect on the nasal mucosa in comparison to the AMT solution. For localization of AMT within the cross-sectional slice of nasal mucosa, the Raman spectrum of pure AMT was utilized as a reference. The frequency of occurrence was visually represented in the chemical maps, correlating to the statistical distribution of specific chemical constituents (Fig. 8). Various colors of the chemical map demonstrate the relative intensity change of AMT in each region of the tissue. The red area indicates the availability of AMT in high intensity, while the green area denotes zones that are related to the formulation's components, including water, BSA, and gellan gum; and then the blue part depicts regions with distinct spectral resolution, which are the characteristics of the nasal mucosa tissue (Sipos et al., 2023). The results revealed that in the case of *in situ* gelling AMT formulation, the mucosal distribution correlation maps demonstrated a remarkable Raman intensity in the upper part of nasal mucosa specimens, corresponding to the high content of protein of the nasal epithelial layer. Meanwhile, for AMT solution, strong existence of AMT was detected in the whole cross-section of the nasal mucosa indicating remarkable penetration of drug and presuming high systemic absorption. Notably, the findings were reliable with the results of *ex vivo* permeation studies. Therefore, this investigation indicated that the *in situ* gelling AMT formulations is instead in the mucosa surface than permeating across the nasal mucosa membrane; therefore, it could be suitable for treating a local infection in the nasal cavity.

Based on the findings presented here, it is clear that the formulation of mucoadhesive *in situ* nasal gel of amoxicillin trihydrate was able to provide great potential for local treatment in nasal mucosa. The formulation of GG0.3 % showed proper characteristics based on the reconstitution time, mucoadhesive properties, and the ability to retain the drug. In the future, it is essential that more thorough research be done to guarantee the usability of this delivery system.

4. Conclusion

The utilization of *in situ* gelling system could be a promising approach to effectively administer AMT via nasal delivery route for treating local infections within the nasal passages, such as ABR. Accordingly, it is of great importance to carry out *ex vivo* mucosal permeation and retention studies, to ensure the application of nasal formulation is in alignment with its therapeutic purposes. In this work, noteworthy outcomes were attained concerning crucial characteristics of nasal formulation, which in this case, the *in situ* gelling AMT

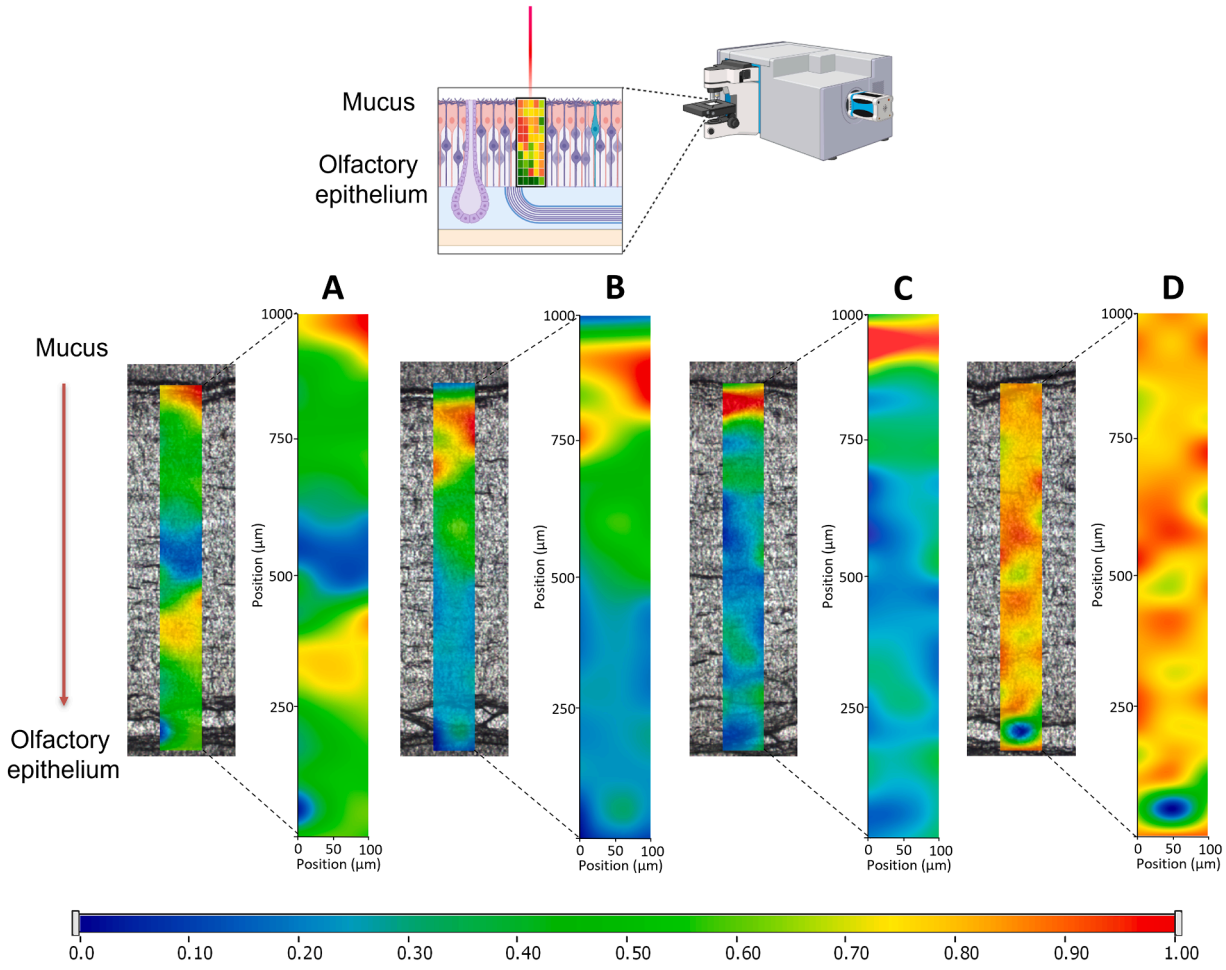

Fig. 8. Raman correlation mapping of the *in situ* gelling AMT formulations: (A) GG0.2 %, (B) GG0.3 %, and (C) GG0.4 %, in comparison to (D) AMT solution (1 mg/ml).

formulations exhibited proper mucoadhesive properties, facilitating the formulation to stay longer in nasal cavity. Moreover, the *in situ* gelling AMT formulation containing 0.3 % of GG was selected as a suitable polymer concentration by considering all essential results. Interestingly, the *ex vivo* permeability and retention studies revealed that all *in situ* gelling AMT formulations were able to retain the drug on the surface of the human nasal mucosa tissue instead of directly penetrating through the membrane, confirming its potential for treating nasal infections locally. In summary, this work demonstrates that the *in situ* gelling systems exhibited potential as a delivery vehicle for improved nasal applicability of AMT for local therapeutic purpose. Further, more thorough investigations should be taken into account to intensively explore the potential of this delivery systems for nasal application.

Funding

The publication was funded by The University of Szeged Open Access Fund (FundRef, Grant No. 6940).

CRediT authorship contribution statement

Sandra Aulia Mardikasari: Writing – original draft, Visualization, Software, Methodology, Investigation, Conceptualization. **Gábor Katona:** Writing – review & editing, Visualization, Supervision, Project administration, Methodology, Formal analysis, Data curation, Conceptualization. **Mária Budai-Szűcs:** Validation, Methodology, Investigation. **Ágnes Kiricsi:** Validation, Methodology, Investigation. **László Rovó:** Validation, Resources, Methodology. **Ildikó Csóka:** Writing – review & editing, Validation, Supervision, Project administration, Funding acquisition, Formal analysis, Conceptualization.

Declaration of competing interest

The authors declare no conflict of interest.

Data availability

Data will be made available on request.

Acknowledgment

This work was supported by Project no. TKP2021-EGA-32 implemented with support provided by the Ministry of Innovation and Technology of Hungary from the National Research, Development, and Innovation Fund, financed under the TKP2021-EGA funding scheme and by János Bolyai Research Scholarship of the Hungarian Academy of Sciences (G. Katona, BO/00251/21).

References

Agrawal, M., Saraf, S., Saraf, S., Dubey, S.K., Puri, A., Gupta, U., Kesharwani, P., Ravichandiran, V., Kumar, P., Naidu, V.G.M., Murty, U.S., Ajazuddin, Alexander, A., 2020. Stimuli-responsive *in situ* gelling system for nose-to-brain drug delivery. J. Control. Release 327, 235–265. https://doi.org/10.1016/j.jconrel.2020.07.044.

Amighi, F., Emam-Djomeh, Z., Labbafi-Mazraeh-Shahi, M., 2020. Effect of different cross-linking agents on the preparation of bovine serum albumin nanoparticles. J. Iran. Chem. Soc. 17, 1223–1235. https://doi.org/10.1007/s13738-019-01850-9.

Arana, L., Gallego, L., Alkorta, I., 2021. Incorporation of antibiotics into solid lipid nanoparticles: a promising approach to reduce antibiotic resistance emergence. Nanomaterials 11, 1–27. https://doi.org/10.3390/nano11051251.

Axiotakis, L.G., Szeto, B., Gonzalez, J.N., Caruana, F.F., Gudis, D.A., Overdevest, J.B., 2022. Antibiotic adverse effects in pediatric acute rhinosinusitis: systematic review and meta-analysis. Int. J. Pediatr. Otorhinolaryngol. 156, 111064 https://doi.org/10.1016/j.ijporl.2022.111064.

Bartos, C., Szabó-Révész, P., Horváth, T., Varga, P., Ambrus, R., 2021. Comparison of modern *in vitro* permeability methods with the aim of investigation nasal dosage forms. Pharmaceutics 13. https://doi.org/10.3390/pharmaceutics13060846.

Beech, K.E., Biddlecombe, J.G., Van Der Walle, C.F., Stevens, L.A., Rigby, S.P., Burley, J. C., Allen, S., 2015. Insights into the influence of the cooling profile on the reconstitution times of amorphous lyophilized protein formulations. Eur. J. Pharm. Biopharm. 96, 247–254. https://doi.org/10.1016/j.ejpb.2015.07.029.

Cao, S., Ren, X., Zhang, Q., Chen, E., Xu, F., Chen, J., Liu, L.C., Jiang, X., 2009. *In situ* gel based on gellan gum as new carrier for nasal administration of mometasone furoate. Int. J. Pharm. 365, 109–115. https://doi.org/10.1016/j.ijpharm.2008.08.042.

Cao, W., Krishnan, S., Ricci, M.S.., Shih, L.Y., Liu, D., Gu, J.H.u., Jameel, F., 2013. Rational design of lyophilized high concentration protein formulations-mitigating the challenge of slow reconstitution with multidisciplinary strategies. Eur. J. Pharm. Biopharm. 85, 287–293. https://doi.org/10.1016/j.ejpb.2013.05.001.

Cassanelli, M., Norton, I., Mills, T., 2018. Role of gellan gum microstructure in freeze drying and rehydration mechanisms. Food Hydrocoll. 75, 51–61. https://doi.org/10.1016/j.foodhyd.2017.09.013.

Chen, S., Ashgriz, N., 2022. Droplet size distribution in swirl nozzles. Int. J. Multiph. Flow 156, 104219. https://doi.org/10.1016/j.ijmultiphaseflow.2022.104219.

Chen, X., Yan, J., Yu, S., Wang, P., 2018. Formulation and *in vitro* release kinetics of mucoadhesive blend gels containing matrine for buccal administration. AAPS J 19, 470–480. https://doi.org/10.1208/s12249-017-0853-7.

Chen, Y., Liu, Y., Xie, J., Zheng, Q., Yue, P., Chen, L., Hu, P., Yang, M., 2020. Nose-to-brain delivery by nanosuspensions-based *in situ* gel for breviscapine. Int. J. Nanomedicine 15, 10435–10451. https://doi.org/10.2147/IJN.S265659.

Cingi, C., Bayar Muluk, N., Mitsias, D.I., Papadopoulos, N.G., Klimek, L., Laulajainen-Hongisto, A., Hytönen, M., Toppila-Salmi, S.K., Scadding, G.K., 2021. The nose as a route for therapy: part 1. Pharmacotherapy. Front. Allergy 2, 1–17. https://doi.org/10.3389/falgy.2021.638136.

Cook, S.L., Bull, S.P., Methven, L., Parker, J.K., Khutoryanskiy, V.V., 2017. Food hydrocolloids mucoadhesion: a food perspective. Food Hydrocoll. 72, 281–296. https://doi.org/10.1016/j.foodhyd.2017.05.043.

Dayal, P., Shaik, M.S., Singh, M., 2004. Evaluation of different parameters that affect droplet-size distribution from nasal sprays using the Malvern Spraytec®. J. Pharm. Sci. 93, 1725–1742. https://doi.org/10.1002/jps.20090.

del Castillo-Santaella, T., Aguilera-Garrido, A., Galisteo-González, F., Gálvez-Ruiz, M.J., Molina-Bolívar, J.A., Maldonado-Valderrama, J., 2022. Hyaluronic acid and human/bovine serum albumin shelled nanocapsules: interaction with mucins and *in vitro* digestibility of interfacial films. Food Chem. 383 https://doi.org/10.1016/j.foodchem.2022.132330.

Djupesland, P.G., Skretting, A., 2012. Nasal deposition and clearance in man: comparison of a bidirectional powder device and a traditional liquid spray pump. J. Aerosol Med. Pulm. Drug Deliv. 25, 280–289. https://doi.org/10.1089/jamp.2011.0924.

EMA, 2006. Guideline on the pharmaceutical quality of inhalation and nasal products. London.

Emad, N.A., Ahmed, B., Alhalmi, A., Alzobaidi, N., Al-Kubati, S.S., 2021. Recent progress in nanocarriers for direct nose to brain drug delivery. J. Drug Deliv. Sci. Technol. 64, 1–11. https://doi.org/10.1016/j.jddst.2021.102642.

Enggi, C.K., Isa, H.T., Sulistiawati, S., Ardika, K.A.R., Wijaya, S., Asri, R.M., Mardikasari, S.A., Donnelly, R.F., Permana, A.D., 2021. Development of thermosensitive and mucoadhesive gels of cabotegravir for enhanced permeation and retention profiles in vaginal tissue: a proof of concept study. Int. J. Pharm. 609, 121182 https://doi.org/10.1016/j.ijpharm.2021.121182.

Fiorica, C., Biscari, G., Palumbo, F.S., Pitarresi, G., Martorana, A., Giammona, G., 2021. Physicochemical and rheological characterization of different low molecular weight gellan gum products and derived ionotropic crosslinked hydrogels. Gels 7. https://doi.org/10.3390/gels7020062.

Forier, K., Raemdonck, K., De Smedt, S.C., Demeester, J., Coenye, T., Braeckmans, K., 2014. Lipid and polymer nanoparticles for drug delivery to bacterial biofilms. J. Control. Release 190, 607–623. https://doi.org/10.1016/j.jconrel.2014.03.055.

Furubayashi, T., Inoue, D., Kamaguchi, A., Higashi, Y., Sakane, T., 2007. Influence of formulation viscosity on drug absorption following nasal application in rats. Drug Metab. Pharmacokinet. 22, 206–211. https://doi.org/10.2133/dmpk.22.206.

Gadziński, P., Froelich, A., Jadach, B., Wojtyłko, M., Tatarek, A., Białek, A., Krysztofiak, J., Gackowski, M., Otto, F., Osmałek, T., 2023. Ionotropic gelation and chemical crosslinking as methods for fabrication of modified-release gellan gum-based drug delivery systems. Pharmaceutics 15, 1–34. https://doi.org/10.3390/pharmaceutics15010108.

Gao, M., Shen, X., Mao, S., 2020. Factors influencing drug deposition in the nasal cavity upon delivery via nasal sprays. J. Pharm. Investig. 50, 251–259. https://doi.org/10.1007/s40005-020-00482-z.

Gao, W., Thamphiwatana, S., Angsantikul, P., Zhang, L., 2014. Nanoparticle approaches against bacterial infections. Wiley Interdiscip. Rev. Nanomedicine Nanobiotechnology 6, 532–547. https://doi.org/10.1002/wnan.1282.

Gholizadeh, H., Cheng, S., Pozzoli, M., Messerotti, E., Traini, D., Young, P., Kourmatzis, A., Ong, H.X., 2019. Smart thermosensitive chitosan hydrogel for nasal delivery of ibuprofen to treat neurological disorders. Expert Opin. Drug Deliv. 16, 453–466. https://doi.org/10.1080/17425247.2019.1597051.

Hao, J., Zhao, J., Zhang, S., Tong, T., Zhuang, Q., Jin, K., Chen, W., Tang, H., 2016. Fabrication of an ionic-sensitive *in situ* gel loaded with resveratrol nanosuspensions intended for direct nose-to-brain delivery. Colloids Surf. B Biointerfaces 147, 376–386. https://doi.org/10.1016/j.colsurfb.2016.08.011.

Hosny, K.M., Hassan, A.H., 2014. Intranasal *in situ* gel loaded with saquinavir mesylate nanosized microemulsion: preparation, characterization, and *in vivo* evaluation. Int. J. Pharm. 475, 191–197. https://doi.org/10.1016/j.ijpharm.2014.08.064.

Huang, G., Xie, J., Shuai, S., Wei, S., Chen, Y., Guan, Z., Zheng, Q., Yue, P., Wang, C., 2021a. Nose-to-brain delivery of drug nanocrystals by using Ca2+ responsive deacetylated gellan gum based *in situ*-nanogel. Int. J. Pharm. 594, 120182 https://doi.org/10.1016/j.ijpharm.2020.120182.

Huang, G., Xie, J., Shuai, S., Wei, S., Chen, Y., Guan, Z., Zheng, Q., Yue, P., Wang, C., 2021b. Nose-to-brain delivery of drug nanocrystals by using Ca2+ responsive

deacetylated gellan gum based *in situ*-nanogel. Int. J. Pharm. 594, 120182 https://doi.org/10.1016/j.ijpharm.2020.120182.
Hurtta, M., Pitkänen, I., Knuutinen, J., 2004. Melting behaviour of D-sucrose, D-glucose and D-fructose. Carbohydr. Res. 339, 2267–2273. https://doi.org/10.1016/j.carres.2004.06.022.
Huttner, A., Bielicki, J., Clements, M.N., Frimodt-Møller, N., Muller, A.E., Paccaud, J.P., Mouton, J.W., 2020. Oral amoxicillin and amoxicillin–clavulanic acid: properties, indications and usage. Clin. Microbiol. Infect. 26, 871–879. https://doi.org/10.1016/j.cmi.2019.11.028.
Illum, L., 2006. Nasal clearance in health and disease. J. Aerosol Med. 19, 92–99.
Inoue, D., Tanaka, A., Kimura, S., Kiriyama, A., Katsumi, H., Yamamoto, A., Ogawara, K., Kimura, T., Higaki, K., Yutani, R., Sakane, T., Furubayashi, T., 2018. The relationship between *in vivo* nasal drug clearance and *in vitro* nasal mucociliary clearance: application to the prediction of nasal drug absorption. Eur. J. Pharm. Sci. 117, 21–26. https://doi.org/10.1016/j.ejps.2018.01.032.
Jullaphant, T., Nakpeng, T., Srichana, T., 2019. Montelukast nasal spray: formulation development and *in vitro* evaluation. Pharm. Dev. Technol. 24, 494–503. https://doi.org/10.1080/10837450.2018.1514523.
Kakati, N., Parashar, C.K., Thakur, S., Deshmukh, O.S., Bandyopadhyay, D., 2022. Microrheology of Mucin-Albumin Assembly Using Diffusing Wave Spectroscopy. ACS Appl. Bio Mater. https://doi.org/10.1021/acsabm.2c00098.
Karimi, M., Bahrami, S., Ravari, S.B., Zangabad, P.S., Mirshekari, H., Bozorgomid, M., Shahreza, S., Sori, M., Hamblin, M.R., 2016. Albumin nanostructures as advanced drug delivery systems. Expert Opin. Drug Deliv. 13, 1609–1623. https://doi.org/10.1080/17425247.2016.1193149.
Katona, G., Balogh, G.T., Dargó, G., Gáspár, R., Márki, Á., Ducza, E., Sztojkov-Ivanov, A., Tömösi, F., Kecskeméti, G., Janáky, T., Kiss, T., Ambrus, R., Pallagi, E., Szabó-Révész, P., Csóka, I., 2020. Development of meloxicam-human serum albumin nanoparticles for nose-to-brain delivery via application of a quality by design approach. Pharmaceutics 12. https://doi.org/10.3390/pharmaceutics12020097.
Katona, G., Sabir, F., Sipos, B., Naveed, M., Schelz, Z., Zupkó, I., Csóka, I., 2022. Development of lomustine and n-propyl gallate Co-encapsulated liposomes for targeting glioblastoma multiforme via intranasal administration. Pharmaceutics 14. https://doi.org/10.3390/pharmaceutics14030631.
Katona, G., Sipos, B., Budai-Szűcs, M., Balogh, G.T., Veszelka, S., Gróf, I., Deli, M.A., Volk, B., Szabó-Révész, P., Csóka, I., 2021. Development of *in situ* gelling meloxicam-human serum albumin nanoparticle formulation for nose-to-brain application. Pharmaceutics 13, 1–22. https://doi.org/10.3390/pharmaceutics13050646.
Keller, L.A., Merkel, O., Popp, A., 2021. Intranasal drug delivery: opportunities and toxicologic challenges during drug development. Drug Deliv. Transl. Res. https://doi.org/10.1007/s13346-020-00891-5.
Khutoryanskiy, V.V., 2011. Advances in Mucoadhesion and Mucoadhesive Polymers. Macromol. Biosci. 11, 748–764. https://doi.org/10.1002/mabi.201000388.
Kianfar, E., 2021. Protein nanoparticles in drug delivery: animal protein, plant proteins and protein cages, albumin nanoparticles. J. Nanobiotechnology 19, 1–32. https://doi.org/10.1186/s12951-021-00896-3.
Kiss, T., Ambrus, R., Abdelghafour, M.M., Zeiringer, S., Selmani, A., Roblegg, E., Budai-Szűcs, M., Janovák, L., Lőrinczi, B., Deák, Á., Bernkop-Schnürch, A., Katona, G., 2022. Preparation and detailed characterization of the thiomer chitosan–cysteine as a suitable mucoadhesive excipient for nasal powders. Int. J. Pharm. 626 https://doi.org/10.1016/j.ijpharm.2022.122188.
Kolawole, O.M., Cook, M.T., 2023. *In situ* gelling drug delivery systems for topical drug delivery. Eur. J. Pharm. Biopharm. 184, 36–49. https://doi.org/10.1016/j.ejpb.2023.01.007.
Kramm, K., Orth, M., Teiwes, A., Kammerhofer, J.C., Meunier, V., Pietsch-Braune, S., Heinrich, S., 2023. Influence of nozzle parameters on spray pattern and droplet characteristics for a two-fluid nozzle. Chem. Ing.-Tech. 95, 151–159. https://doi.org/10.1002/cite.202200152.
Kulkarni, S.S., Patel, S.M., Bogner, R.H., 2020. Reconstitution Time for Highly Concentrated Lyophilized Proteins: role of Formulation and Protein. J. Pharm. Sci. 109, 2975–2985. https://doi.org/10.1016/j.xphs.2020.05.029.
Kulkarni, S.S., Suryanarayanan, R., Rinella, J.V., Bogner, R.H., 2018. Mechanisms by which crystalline mannitol improves the reconstitution time of high concentration lyophilized protein formulations. Eur. J. Pharm. Biopharm. 131, 70–81. https://doi.org/10.1016/j.ejpb.2018.07.022.
Kundoor, V., Dalby, R.N., 2011. Effect of formulation- and administration-related variables on deposition pattern of nasal spray pumps evaluated using a nasal cast. Pharm. Res. 28, 1895–1904. https://doi.org/10.1007/s11095-011-0417-6.
Le Guellec, S., Ehrmann, S., Vecellio, L., 2021. *In vitro – in vivo* correlation of intranasal drug deposition. Adv. Drug Deliv. Rev. 170, 340–352. https://doi.org/10.1016/j.addr.2020.09.002.
Lemiengre, M., van Driel, M., Merestein, D., Liira, H., Makela, M., De Sutter, A.I., 2018. Antibiotics for acute rhinosinusitis in adults (review). Cochrane Database Syst. Rev. 2018, 1–80. https://doi.org/10.1002/14651858.CD006089.pub5.
Loureiro, A., G. Azoia, N., C. Gomes, A., Cavaco-Paulo, A., 2016. Albumin-based nanodevices as drug carriers. Curr. Pharm. Des. 22, 1371–1390. https://doi.org/10.2174/1381612822666160125114900.
Lungare, S., Bowen, J., Badhan, R., 2016. Development and evaluation of a novel intranasal spray for the delivery of amantadine. J. Pharm. Sci. 105, 1209–1220. https://doi.org/10.1016/j.xphs.2015.12.016.
Luo, W.C., O'Reilly Beringhs, A., Kim, R., Zhang, W., Patel, S.M., Bogner, R.H., Lu, X., 2021. Impact of formulation on the quality and stability of freeze-dried nanoparticles. Eur. J. Pharm. Biopharm. 169, 256–267. https://doi.org/10.1016/j.ejpb.2021.10.014.
Luoma, J., Lim, F.J., 2020. Strategies to reduce reconstitution time of lyophilized biotherapeutics. J. Pharm. Sci. 109, 1905–1911. https://doi.org/10.1016/j.xphs.2020.02.019.
Mardikasari, S.A., Budai-Szűcs, M., Orosz, L., Burián, K., Csóka, I., Katona, G., 2022a. Development of thermoresponsive-gel-matrix-embedded amoxicillin trihydrate-loaded bovine serum albumin nanoparticles for local intranasal therapy. Gels 8. https://doi.org/10.3390/gels8110750.
Mardikasari, S.A., Katona, G., Budai-Szűcs, M., Sipos, B., Orosz, L., Burián, K., Rovo, L., Csóka, I., 2023a. Quality by design-based optimization of *in situ* ionic-sensitive gels of amoxicillin-loaded bovine serum albumin nanoparticles for enhanced local nasal delivery. Int. J. Pharm. 645 https://doi.org/10.1016/j.ijpharm.2023.123435.
Mardikasari, S.A., Katona, G., Sipos, B., Ambrus, R., Csóka, I., 2023b. Preparation and optimization of bovine serum albumin nanoparticles as a promising gelling system for enhanced nasal drug administration. Gels 9. https://doi.org/10.3390/gels9110896.
Mardikasari, S.A., Sipos, B., Csóka, I., Katona, G., 2022b. Nasal route for antibiotics delivery: advances, challenges and future opportunities applying the quality by design concepts. J. Drug Deliv. Sci. Technol. 77, 1–18. https://doi.org/10.1016/j.jddst.2022.103887.
Matricardi, P., Cencetti, C., Ria, R., Alhaique, F., Coviello, T., 2009. Preparation and characterization of novel Gellan gum hydrogels suitable for modified drug release. Molecules 14, 3376–3391. https://doi.org/10.3390/molecules14093376.
Nazli, A., He, D.L., Liao, D., Khan, M.Z.I., Huang, C., He, Y., 2022. Strategies and progresses for enhancing targeted antibiotic delivery. Adv. Drug Deliv. Rev. 189, 114502 https://doi.org/10.1016/j.addr.2022.114502.
Obaidat, R., Al-Ghzawi, B., Al-Taani, B., Al-Shar'i, N., 2022. Co-crystallization of amoxicillin trihydrate and potassium clavulanate provides a promising approach for preparation of sustained-release microspheres. AAPS PharmSciTech 23. https://doi.org/10.1208/s12249-022-02273-1.
Permana, A.D., Utomo, E., Pratama, M.R., Amir, M.N., Anjani, Q.K., Mardikasari, S.A., Sumarheni, S., Himawan, A., Arjuna, A., Usmanengsi, U., Donnelly, R.F., 2021. Bioadhesive-thermosensitive *in situ* vaginal gel of the gel flake-solid dispersion of itraconazole for enhanced antifungal activity in the treatment of vaginal candidiasis. ACS Appl. Mater. Interfaces 13, 18128–18141. https://doi.org/10.1021/acsami.1c03422.
Protopapa, C., Siamidi, A., Pavlou, P., Vlachou, M., 2022. Excipients used for modified nasal drug delivery: a mini-review of the recent advances. Materials 15. https://doi.org/10.3390/ma15196547 (Basel).
Pu, Y., Goodey, A.P., Fang, X., Jacob, K., 2014. A comparison of the deposition patterns of different nasal spray formulations using a nasal cast. Aerosol Sci. Technol. 48, 930–938. https://doi.org/10.1080/02786826.2014.931566.
Rosenfeld, R.M., 2016. Acute sinusitis in adults. N. Engl. J. Med. 375, 962–970. https://doi.org/10.1056/nejmcp1601749.
Rosenfeld, R.M., Piccirillo, J.F., Chandrasekhar, S.S., Brook, I., Ashok Kumar, K., Kramper, M., Orlandi, R.R., Palmer, J.N., Patel, Z.M., Peters, A., Walsh, S.A., Corrigan, M.D., 2015. Clinical practice guideline (update): adult sinusitis. Otolaryngol. Head Neck Surg. 152, S1–S39. https://doi.org/10.1177/0194599815572097 (United States).
Rovelsky, S.A., Remington, R.E., Nevers, M., Pontefract, B., Hersh, A.L., Samore, M., Madaras-Kelly, K., 2021. Comparative effectiveness of amoxicillin *versus* amoxicillin-clavulanate among adults with acute sinusitis in emergency department and urgent care settings. J. Am. Coll. Emerg. Physicians Open 2, 1–8. https://doi.org/10.1002/emp2.12465.
Salunke, S.R., Patil, S.B., 2016. Ion activated *in situ* gel of gellan gum containing salbutamol sulphate for nasal administration. Int. J. Biol. Macromol. 87, 41–47. https://doi.org/10.1016/j.ijbiomac.2016.02.044.
Sanz, R., Clares, B., Mallandrich, M., Suñer-Carbó, J., Montes, M.J., Calpena, A.C., 2018. Development of a mucoadhesive delivery system for control release of doxepin with application in vaginal pain relief associated with gynecological surgery. Int. J. Pharm. 535, 393–401. https://doi.org/10.1016/j.ijpharm.2017.11.027.
Scherließ, R., 2020. Nasal formulations for drug administration and characterization of nasal preparations in drug delivery. Ther. Deliv. 11, 183–191. https://doi.org/10.4155/tde-2019-0086.
Singh, P., Singh, H., Castro-Aceituno, V., Ahn, S., Kim, Y.J., Yang, D.C., 2017. Bovine serum albumin as a nanocarrier for the efficient delivery of ginsenoside compound K: preparation, physicochemical characterizations and *in vitro* biological studies. RSC Adv 7, 15397–15407. https://doi.org/10.1039/c6ra25264h.
Sipos, B., Bella, Z., Gróf, I., Veszelka, S., Deli, M.A., Szűcs, K.F., Sztojkov-Ivanov, A., Ducza, E., Gáspár, R., Kecskeméti, G., Janáky, T., Volk, B., Budai-Szűcs, M., Ambrus, R., Szabó-Révész, P., Csóka, I., Katona, G., 2023. Soluplus® promotes efficient transport of meloxicam to the central nervous system via nasal administration. Int. J. Pharm. 632 https://doi.org/10.1016/j.ijpharm.2023.122594.
Sipos, B., Katona, G., Csóka, I., 2021. A systematic, knowledge space-based proposal on quality by design-driven polymeric micelle development. Pharmaceutics 13, 1–17. https://doi.org/10.3390/pharmaceutics13050702.
Sipos, B., Szabó-Révész, P., Csóka, I., Pallagi, E., Dobó, D.G., Bélteky, P., Kónya, Z., Deák, Á., Janovák, L., Katona, G., 2020. Quality by design based formulation study of meloxicam-loaded polymeric micelles for intranasal administration. Pharmaceutics 12, 1–29. https://doi.org/10.3390/pharmaceutics12080697.
Snidvongs, K., Thanaviratananich, S., 2017. Update on intranasal medications in rhinosinusitis. Curr. Allergy Asthma Rep. 17 https://doi.org/10.1007/s11882-017-0720-3.
Syed, M.A., Hanif, S., Ain, N., Syed, H.K., Zahoor, A.F., Khan, I.U., Abualsunun, W.A., Jali, A.M., Qahl, S.H., Sultan, M.H., Madkhali, O.A., Ahmed, R.A., Abbas, N., Hussain, A., Qayyum, M.A., Irfan, M., 2022. Assessment of binary agarose – carbopol

buccal gels for mucoadhesive drug delivery : *ex vivo* and *in vivo* characterization. Molecules 27, 1–20. https://doi.org/10.3390/molecules27207004.

Taweel, M.M.E., Aboul-Einien, M.H., Kassem, M.A., Elkasabgy, N.A., 2021. Intranasal zolmitriptan-loaded bilosomes with extended nasal mucociliary transit time for direct nose to brain delivery. Pharmaceutics 13. https://doi.org/10.3390/pharmaceutics13111828.

Trenkel, M., Scherließ, R., 2021. Nasal powder formulations: *in-vitro* characterisation of the impact of powders on nasal residence time and sensory effects. Pharmaceutics 13. https://doi.org/10.3390/pharmaceutics13030385.

Trows, S., Wuchner, K., Spycher, R., Steckel, H., 2014. Analytical challenges and regulatory requirements for nasal drug products in Europe and the U.S. Pharmaceutics 6, 195–219. https://doi.org/10.3390/pharmaceutics6020195.

Velde, F.D., Winter, B.C.M.D., Koch, B.C.P., Gelder, T.V, Mouton, J.W., 2016. Non-linear absorption pharmacokinetics of amoxicillin : consequences for dosing regimens and clinical breakpoints. J. Antimicrob. Chemother. 71, 2909–2917. https://doi.org/10.1093/jac/dkw226.

Verekar, R.R., Gurav, S.S., Bolmal, U., 2020. Thermosensitive mucoadhesive *in situ* gel for intranasal delivery of Almotriptan malate: formulation, characterization, and evaluation. J. Drug Deliv. Sci. Technol. 58, 101778 https://doi.org/10.1016/j.jddst.2020.101778.

Wu, S., 2007. Calculation of interfacial tension in polymer systems. J. Polym. Sci. C Polym. Symp. 34, 19–30. https://doi.org/10.1002/polc.5070340105.

Yeh, Y.C., Huang, T.H., Yang, S.C., Chen, C.C., Fang, J.Y., 2020. Nano-based drug delivery or targeting to eradicate bacteria for infection mitigation: a review of recent advances. Front. Chem. 8, 1–22. https://doi.org/10.3389/fchem.2020.00286.

Youssef, N.A.H.A., Kassem, A.A., Farid, R.M., Ismail, F.A., EL-Massik, M.A.E., Boraie, N. A., 2018. A novel nasal almotriptan loaded solid lipid nanoparticles in mucoadhesive *in situ* gel formulation for brain targeting: preparation, characterization and *in vivo* evaluation. Int. J. Pharm. 548, 609–624. https://doi.org/10.1016/j.ijpharm.2018.07.014.

Yu, Y.S., AboulFotouh, K., Xu, H., Williams, G., Suman, J., Cano, C., Warnken, Z.N., Wu, K.C.W., Williams, R.O., Cui, Z., 2023. Feasibility of intranasal delivery of thin-film freeze-dried, mucoadhesive vaccine powders. Int. J. Pharm. 640, 122990 https://doi.org/10.1016/j.ijpharm.2023.122990.

Zazo, H., Colino, C.I., Lanao, J.M., 2016. Current applications of nanoparticles in infectious diseases. J. Control. Release 224, 86–102. https://doi.org/10.1016/j.jconrel.2016.01.008.